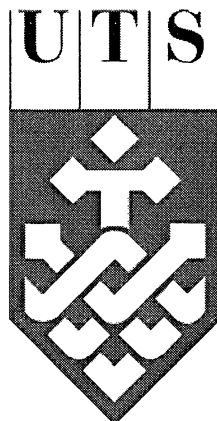


Linearisation, Error Correction Coding and Equalisation for Multi-Level Modulation Schemes

A thesis
submitted in fulfilment
of the requirements for the degree
of
Doctor of Philosophy
at the
University of Technology, Sydney
by

YounSik KIM

Department of Information & Communication Group, Faculty of Engineering



P.O. Box 123, Broadway, NSW 2007, Australia (yskim@eng.uts.edu.au)

March 29, 2005

Certificate of Authorship/Originality

I certify that the work in this thesis has not previously been submitted for a degree nor has it been submitted as part of requirements for a degree except as fully acknowledged within the text.

I also certify that the thesis has been written by me. Any help that I have received in my research work and the preparation of the thesis itself has been acknowledged. In addition, I certify that all information sources and literature used are indicated in the thesis.

Signature of Candidate



April 14, 2005

Abstract

Orthogonal frequency division multiplexing (OFDM) has been standardised for digital audio broadcasting (DAB), digital video broadcasting (DVB) and wireless local area networks (WLAN). OFDM systems are capable of effectively coping with frequency-selective fading without using complex equalisation structures. The modulation and demodulation processes using fast fourier transform (FFT) and its inverse (IFFT) can be implemented very efficiently. More recently, multicarrier code division multiple access (MC-CDMA) based on the combination of OFDM and conventional CDMA has received growing attention in the field of wireless personal communication and digital multimedia broadcasting. It can cope with channel frequency selectivity due to its own capabilities of overcoming the asynchronous nature of multimedia data traffic and higher capacity over conventional multiple access techniques.

On the other hand, multicarrier modulation schemes are based on the transmission of a given set of signals on large numbers of orthogonal subcarriers. Due to the fact that the multicarrier modulated (MCM) signal is a superposition of many amplitude modulated sinusoids, its probability density function is nearly Gaussian. Therefore, the MCM signal is characterised by a very high peak-to-average power ratio (PAPR). As a result of the high PAPR, the MCM signal is severely distorted when a nonlinear high power amplifier (HPA) is employed to obtain sufficient transmitting power. This is very common in most communication systems, and decreases the performance significantly. The simplest way to avoid the nonlinear distortion is substantial output backoff (OBO) operating in the

linear region of the HPA. However, because of the high OBO, the peak transmit power has to be decreased. For this reason, many linearisation techniques have been proposed to compensate for the nonlinearity without applying high OBO. The predistortion techniques have been known and studied as one of the most promising means to solve the problem. In this thesis, an improved memory mapping predistortion technique devised to reduce the large computational complexity of a fixed point iterative (FPI) predistorter is proposed, suitable especially for multicarrier modulation schemes. The proposed memory mapping predistortion technique is further extended to compensate for nonlinear distortion with memory caused by a shaping linear filter. The case of varying HPA characteristics is also considered by using an adaptive memory mapping predistorter which updates the lookup table (LUT) and counteracts these variations. Finally, an amplitude memory mapping predistorter is presented to reduce the LUT size.

Channel coding techniques have been widely used as an effective solution against channel fading in wireless environments. Amongst these, particular attention has been paid to turbo codes due to their performance being close to the Shannon limit. In-depth study and evaluation of turbo coding has been carried out for constant envelope signaling systems such as BPSK, QPSK and M-ary PSK. In this thesis, the performance of TTCM-OFDM systems with high-order modulation schemes, e.g. 16-QAM and 64-QAM, is investigated and compared with conventional channel coding schemes such as Reed-Solomon and convolutional coding. The analysis is performed in terms of spectral efficiency over a multipath fading channel and in presence of an HPA. Maximum a-priori probability (MAP), soft output Viterbi algorithm (SOVA) and pragmatic algorithms are compared for non-binary turbo decoding with these systems. For this setup, iterative multiuser detection in TTCM/MC-CDMA systems with M -QAM is introduced and investigated, adopting a set of random codes to decrease the PAPR. As another application of TTCM, the performance of multicode CDMA systems with TTCM for outer coding over multipath fading channels is investigated.

To achieve a high channel coding gain, received signals have to be equalised to eliminate

intersymbol interference (ISI) at the receiver. Equalisation for OFDM systems is most commonly performed in the frequency domain through least mean squares (LMS) and proportional approaches. In this thesis, an improved LMS equalisation is proposed and compared to the performance of a conventional LMS equaliser. Computer simulations confirm that the performance of the modified LMS equaliser achieves faster convergence and better bit error rate (BER) performance than the conventional one. Turbo equalisation, which is based on a combination of turbo decoding and equalisation, has recently been studied in near optimum receivers for a binary transmission case. This thesis looks into the performance of TTCM-equalisation (TTCM with a MAP equaliser) for M -ary QAM. Algorithm complexity is further reduced by utilising modified MAP equalisation with blind channel estimation by expectation maximisation (EM). This structural improvement is achieved by sharing common information amongst both algorithms. Finally, a blind TTCM-equalisation technique for M -QAM in an unknown channel is introduced and its performance is compared to the case of a known channel.

Acknowledgements

I would like to thank my supervisor, A/Prof. Sam Reisenfeld, for his valuable ideas, suggestions, constructive discussions and guidance in preparing this thesis during a difficult time. Moreover, my gratitude goes to the members of the Cooperative Research Center for Satellite System (CRCSS) and my fellow PhD students for offering help and friendly advice throughout my research. Finally, I am very grateful to my wife and the role she has played in my life supporting me as PhD student in a foreign country - she is the reason that my research is successful. She has always been my closest friend and encouraged me through her dedication and patience when I needed it most.

List of Acronym

AM:	Amplitude Modulation
APP:	A Posteriori Probability
AWGN:	Additive White Gaussian Noise
BCH:	Bose Chaudhuri Hocquenghem
BCJR:	Bahl Cocke Jelinek Rajiv
BER:	Bit Error Rate
BPSK:	Binary Phase Shift Keying
DAB:	Digital Audio Broadcasting
DS-CDMA:	Direct Sequence Code Division Multiple Access
DSP:	Digital Signal Processing
DVB:	Digital Video Broadcasting
EGC:	Equal Gain Combining
EM:	Expectation Maximization
EQ:	Equalizer
FEC:	Forward Error Correction
FFT:	Fast Fourier Transform
FPI:	Fixed Point Iteration
GF:	Galois Field
HPA:	High Power Amplifier
IBO:	Input Back Off
ICI:	Inter Carrier Interference

IFFT:	Inverse Fast Fourier Transform
IMT 2000:	International Mobile Telecommunication 2000
ISI:	Inter Symbol Interference
LLR:	Log Likelihood Ratio
LMS:	Least Mean Square
LUT:	Look Up Table
MAP:	Maximum A priori Probability
MC-CDMA:	Multi Carrier Code Division Multiple Access
MCM:	Multi Carrier Modulation
ML-MD:	Maximum Likelihood Multi user Detection
MMSE:	Minimum Mean Square Error
MRC:	Maximum Ratio Combining
MRC-MUD:	Maximum Ratio Combining Multi User Detection
MSE:	Mean Square Error
OBO:	Output Back Off
OFDM:	Orthogonal Frequency Division Multiplexing
PAPR:	Peak to Average Power Ratio
PD:	Pre Distorter
PDF:	Probability Density Function
PM:	Phase Modulation
PN:	Pseudorandom Noise
PSK:	Phase Shift Keying
QAM:	Quadrature Amplitude Modulation
RAM:	Random Access Memory
RDP:	Ram Data Point
RMSE:	Root Mean Square Error
RS:	Reed Solomon
SISO:	Soft Input Soft Output
SNR:	Signal to Noise Ratio

SOVA:	Soft Output Viterbi Algorithm
SSPA:	Solid State Power Amplifier
TCM:	Trellis Coded Modulation
TD:	Total Degradation
TTCM:	Turbo Trellis Coded Modulation
TWTA:	Travelling Wave Tube Amplifier
VA:	Viterbi Algorithm
VLSI:	Very Large Scale Integrated
WLAN:	Wireless Local Area Network

List of Symbols

$A(\cdot)$	Amplitude of a HPA output
A_{MAT}	Autocorrelation matrix used for the EM algorithm
A_{RAM}	RAM memory address used for the memory mapping predistorter
$A_{\text{sat,I}}$	Maximum input saturation power
$A_{\text{sat,O}}$	Maximum output saturation power
b_k	k -th bit
B	Block size
C_{EQ}	Equaliser coefficients
C_{ORG}	Second orthogonal code used for multicode CDMA systems
C_{PAPR}	Random code used for MC-CDMA systems to reduce PAPR
C_{VEC}	Cross-correlation matrix used for the EM algorithm
$\text{DET} \cdot :$	Determinant of matrix
D_{VEC}	Decision vector used for RS decoding
e	Error value used for LMS equalisation
E_a	Estimated average symbol energy in a Rayleigh fading channel
El_m	Error location value used for RS decoding
d_k	k -th symbol
D_{CON}	Convolutional Depth, which is the number of symbols given to decode one symbol at the convolutional decoder
f_c	Carrier frequency (RF)
G_{MC}	Processing gain of multicode CDMA systems
g	Linear gain of a HPA

$g_{\text{GF}}(D)$:	Polynomial function
H	Channel coefficients vector in frequency domain
I	Number of iteration used for iterative decoding
$Im\{\cdot\}$	Imaginary part of a complex value.
K_{SYM}	K -number of symbols
K_b	the number of bits
K_{CON}	Constraint length for a recursive encoder
L	Number of coefficients of a linear filter
La_k^{e2}	k -th a priori probability to decoder 2
Le_k^{e1}	k -th extrinsic information from decoder 1
$\text{Map}(\cdot)$	Channel mapping function
M_{LUT}	Look-up table (LUT) size
M_{PATH}	Path matrix used for the SOVA algorithm
M_{sym}	Number of symbols for M -ary QAM
N_{FFT}	The number of FFT points
N_p	First orthogonal code length of a multicode-CDMA system
N_{POS}	Position number used for S-interleaver
N_w	First orthogonal code length of a multicode-CDMA system
$O(\cdot)$	Output of a predistorter
P_e	Bit error probability
$p_T(\cdot)$	a unity rectangular function
\mathbf{P}_{IN}	Average HPA input signal power
\mathbf{P}_{OUT}	Average output signal power
$P(X_k = d_k)$	Log likelihood probability used for EM algorithm
$r_1^{K_{\text{sym}}}$	K_{sym} number of received symbols
R	Data rate
$Re\{\cdot\}$	Real part of a complex value.
S	Number of status
$S_{m,\text{SYN}}$	m -th syndrome used for Reed-Solomon code

T_b	Bit duration
T_c	Chip duration of CDMA systems
T_d	Propagation delay of a multipath channel
t_{ER}	Number of error correction for Reed-Solomon code
T_{FFT}	FFT integration period
T_{GI}	Guard interval
T_s	Sampling period
T_{SYM}	Symbol duration
U	Number of users
$W[n]$	n -th orthogonal code
$x[n]_{\text{Norm}}$	Normalised input to a predistorter
α^{ch}	Channel attenuation factor
$\Phi(\cdot)$	Phase distortion of a nonlinear HPA
ξ	Convergence constant
$\Lambda(\cdot)$	Log-likelihood ratio (LLR)
α_{GF}	A primitive element of $GF(2^m)$
$\alpha_k(s)$	Forward probabilities used for turbo decoding
$\gamma_k(m, s)$	Transition probabilities used for turbo decoding
$\beta_k(s)$	Backward probabilities used for turbo decoding
ψ	a complex Gaussian noise
κ	Number of iterations used for a FPI predistorter
Ψ	a complex Gaussian noise in frequency domain
Δ	Channel mapping values used for iterative multiuser detection
σ_c^2	Channel variance
ζ	a constant used for pragmatic TTCM decoding
\otimes	matrix multiplication

Contents

Certificate	i
Abstract	ii
Acknowledgements	v
List of Acronym	vi
List of Symbols	ix
List of Figures	xxi
1 Introduction	1
1.1 Thesis Overview and Context	1
1.2 Orthogonal Frequency Division Multiplexing	3
1.2.1 Introduction	3
1.2.2 The Basic Principle of OFDM	4
1.3 Multi-Carrier Code Division Multiple Access (MC-CDMA)	8
1.3.1 Introduction	8
1.3.2 The Basic Principle of MC-CDMA	9
1.4 Summary of Contributions	14
2 Predistortion Techniques	16
2.1 Methods to Compensate for Nonlinear Distortion	17
2.2 Model of a High Power Amplifier	19

2.3	The Basic principle of the Predistortion	21
2.4	Review of the Fixed Point Iteration Predistorter	23
2.5	Improvement of the Memory Mapping Predistorter	26
2.6	Adaptive Memory Mapping Predistorter	30
2.7	Trade-Off Between LUT size and Complexity	33
2.8	PAPR of MC-CDMA	35
2.9	Simulation Results	37
2.9.1	OFDM system	37
2.9.2	MC-CDMA system	44
2.9.3	Summary of the simulations	50
3	Coded Multicarrier Modulation Schemes	52
3.1	The Basic Principles of Conventional FEC Codes	53
3.1.1	Reed-Solomon Codes	54
3.1.2	Convolutional Codes	57
3.2	Turbo Trellis Coded Modulation	60
3.2.1	TTCM Encoding	61
3.2.2	Interleaver	63
3.2.3	TTCM Decoding	65
3.3	Coded OFDM systems with Turbo Trellis Coded Modulation	74
3.4	Iterative Multiuser Detection for the MultiCarrier-CDMA systems with multilevel modulation schemes in the presence of a nonlinear HPA	78
3.5	Turbo Coded Multicode CDMA systems with M-QAM in the presence of a nonlinear HPA	85
3.6	Simulation Results and Discussion	91
3.6.1	Coded OFDM systems	92
3.6.2	Coded MultiCarrier-CDMA systems	103
3.6.3	Coded MultiCode-CDMA systems	111
3.6.4	Summary of the simulations	117

4	Equalisation Techniques	119
4.1	The Basic Principle of Equalisation in the Frequency Domain	120
4.2	An Improved Adaptive LMS Equalisation Based on Training Signals . . .	123
4.3	MAP Equalisation	125
4.4	Modified MAP Equalisation for M-ary QAM	126
4.5	EM based Blind Channel Estimation	129
4.6	Turbo Equalisation for M-ary QAM	132
4.7	Blind TTCM Equalisation for M-ary QAM	136
4.8	Simulation Results	140
4.8.1	Equalisation of Binary Modulation	146
4.8.2	Equalisation of M-QAM	147
4.8.3	Summary of the simulations	155
5	Conclusion	156
	Bibliography	159

List of Figures

1.1	A typical OFDM system model	5
1.2	The cyclically extended OFDM symbols in three different carriers at the receiver	6
1.3	A typical structure of a synchronous baseband MC-CDMA system	9
2.1	The basic concept of the predistortion	22
2.2	Predistorter applied to a HPA and a shaping filter	23
2.3	The predistorter based on the FPI	26
2.4	Block diagram of the proposed memory mapping predistorter	30
2.5	The adaptive memory mapping predistorter	31
2.6	Amplitude memory mapping predistorter	33
2.7	Peak-to-average power ratio of MC-CDMA signals (128 Walsh code)	35
2.8	peak-to-average power ratio of the MC-CDMA signals with Walsh and random code	37
2.9	16-QAM Constellation (OBO=6.0, Eb/No=15, $M_{LUT} = 100$)	38
2.10	BER comparison of OFDM systems with FPI and memory mapping predistorter, no linear filter - (1)	39
2.11	BER comparison of OFDM systems with FPI and memory mapping predistorter, no linear filter - (2)	39
2.12	BER comparison of OFDM systems with the FPI and the memory mapping predistorter and with a linear filter - (1)	40

2.13 BER comparison of OFDM systems with the FPI and the memory mapping predistorter and with a linear filter -(2)	41
2.14 Mean square error of the proposed memory mapping predistorter	41
2.15 BER performance of an OFDM system using the proposed memory mapping predistorter and the LUT size as a parameter	42
2.16 Total degradation and mean square error in an OFDM system using the proposed predistorter	43
2.17 Power spectral densities of OFDM HPA output signals using the memory mapping predistorter with a LUT size of $M_{LUT}=100$	44
2.18 Baseband MC-CDMA system using a predistorter and an HPA	45
2.19 BER Performance of a QPSK/MC-CDMA system operating at OBO levels of 0 and 1 dB	46
2.20 BER Performance of a QPSK/MC-CDMA system operating at OBO levels of 2 and 3 dB	46
2.21 BER Performance of QPSK/MC-CDMA systems using a linear filter and a HPA	47
2.22 Total degradation of MC-CDMA systems using the proposed predistorters	48
2.23 BER performance of a 16-QAM/MC-CDMA system, OBO = 2 and 3 dB .	49
2.24 BER Performance of a 16-QAM/MC-CDMA system, OBO = 4 and 5 dB	49
2.25 BER comparison between MC-CDMA systems with and without PAPR minimizing codes (OBO = 5 dB)	50
3.1 Linear feedback shift register (LFSR) RS encoder	55
3.2 A typical rate 1/2 convolutional encoder structure	58
3.3 Trellis diagram with $S=4$ ($K_{CON} = 3$)	60
3.4 A simplified encoder structure of Turbo TCM	61
3.5 Gray mapping for 16-QAM and Ungerboeck mapping for 64-QAM . . .	63
3.6 A typical decoder structure for TTCM	65
3.7 Trellis section	67
3.8 A structure of pragmatic turbo TCM decoder	71

3.9	A baseband coded OFDM system using the predistorter and turbo trellis coded modulation over a nonlinear multipath fading channel	74
3.10	A turbo TCM encoder structure	75
3.11	Turbo Trellis Coded Modulation Encoder for 64-QAM	77
3.12	A baseband synchronous multicarrier-CDMA system with Turbo TCM for uplink	79
3.13	A multipath fading channel model	80
3.14	A typical baseband synchronous MC-CDMA system with a HPA and TTCM for downlink	82
3.15	Structure of a synchronous multicode-CDMA system with predistorter and HPA	86
3.16	Structure of a synchronous multicode-CDMA system with predistorter and HPA for downlink in a mobile communications system	89
3.17	Structure of a Rake receiver using maximum ratio combining (MRC) in time domain. The boxes marked by T_c correspond to the chip duration of the spreading code	90
3.18	BER performance comparison of different turbo decoding algorithms (MAP, SOVA and Log-MAP) in a BPSK system over an AWGN channel .	92
3.19	BER comparison of pragmatic decoding to symbol-by-symbol MAP decoding for TTCM-OFDM systems, 16-QAM, rate $R = 1/2$ (2 bits per symbol) over an AWGN channel, parameter: number of iterations (1, 2, 3, 10)	93
3.20	BER comparison of a 1024-point OFDM systems over an AWGN channel using different mapping methods, 64-QAM, 4-bits/symbol	94
3.21	BER comparison between MAP, SOVA and pragmatic decoding in a 512-point OFDM system over an AWGN channel, 16-QAM, 2-bits/symbol . .	95
3.22	The BER performances of the Turbo TCM/OFDM systems with different order modulation schemes over AWGN channel	95

3.23 BER performance of 16QAM-TTCM-OFDM systems using different block sizes for iterative turbo decoding over AWGN channel	96
3.24 Shannon's Limit plot	97
3.25 BER performance of coded OFDM systems using 16-QAM high-order modulation with Reed Solomon coding and convolutional coding over an AWGN channel	98
3.26 BER performance of two TTCM 512-point FFT OFDM systems with 16-QAM ($R=2$ bits/symbol, $K_{CON}=3$, $I=5120$) and 64-QAM ($R=4$ bits/symbol, $K_{CON}=5$, $I=10240$) in a nonlinear environment	100
3.27 BER performance of TTCM-OFDM systems with an HPA at different OBO levels (2 & 6 dB)	100
3.28 BER comparison of coded OFDM systems with an HPA (OBO = 6 dB) using different channel coding techniques	101
3.29 Various BER comparisons of TTCM-OFDM systems with an HPA in AWGN and Rayleigh fading channels	102
3.30 BER performance of a 16-QAM 512-point FFT TTCM-OFDM systems with an HPA in a Rayleigh multipath fading channel, 2 bits/symbols, interleaver size = 5120, 4 iterations, constraint length = 5	103
3.31 BER performance of TTCM/MC-CDMA systems using M -QAM (16, 64) over AWGN channel	104
3.32 BER comparison of an AWGN and Rayleigh channel for turbo coded MC-CDMA systems using QPSK modulation	105
3.33 BER performance of 16-QAM TTCM/MC-CDMA systems with an HPA (OBO = 6 dB), 2 bits/symbol, AWGN channel	106
3.34 BER performance of a 16-QAM TTCM/MC-CDMA system with MRC combiner, 2 bits/symbol, Rayleigh multipath fading channel	107
3.35 BER comparison between TTCM-MC-CDMA systems with a MRC and a MRC-MUD, 16-QAM, 2 bits/symbol	108

3.36	The simulated BER performance over the number of active users in the TTCM-MC-CDMA systems, $E_b/N_0 = 2dB$	109
3.37	BER performance of a 16-QAM TTCM/MC-CDMA system with MRC combiner and iterative MUD, 2 bits per symbol over a 3-path Rayleigh fading channel (OBO = 2 & 4 dB)	109
3.38	BER performance of 16-QAM TTCM/MC-CDMA systems with a MRC combiner and iterative MUD, 2 bits per symbol over a 3-path Rayleigh fading channel (OBO = 6 & 8 dB)	110
3.39	BER performance of multicode CDMA systems using PN and Walsh Hadamard codes over an AWGN channel	111
3.40	BER versus number of users in a multicode CDMA system over an AWGN channel	112
3.41	Constellation of received 16-QAM multicode-CDMA signals with the predistorter and an HPA ($E_b/N_0 = 20$ [dB] & OBO=6 [dB])	113
3.42	BER performance of multicode CDMA system with 16-QAM in with an HPA over an AWGN channel (OBO = 4 & 8 dB)	113
3.43	BER performance of a coded multicode CDMA system over an AWGN channel	114
3.44	BER performance of a coded multicode CDMA system over a multipath fading channel for uplink case	114
3.45	BER performance of TTCM multicode CDMA system with 16-QAM over a nonlinear multipath channel for uplink case (OBO = 4 & 5 dB)	115
3.46	BER comparison of coded multicode CDMA systems with a HPA over nonlinear multipath fading channels	116
3.47	BER comparison of coded multicode CDMA systems with a HPA and the predistorter over nonlinear multipath fading channels	116
4.1	General baseband OFDM system block diagram with an HPA, equaliser and channel decoder	121
4.2	Transmission model with a linear channel filter	125

4.3	the proposed MAP equaliser using EM algorithm	130
4.4	General structure of a turbo equaliser	133
4.5	Trellis diagrams for the encoder and the ISI channel	134
4.6	Structure of a blind TTCM equaliser for M_{SYM} -QAM	137
4.7	RMS Error and BER performance of the proposed and the conventional LMS equalisers in a 512-point OFDM system with 16-QAM modulation .	140
4.8	Constellations of received 16-QAM signals in an OFDM system with an HPA over an ISI channel ($\text{OBO} = 6 \text{ dB}$, $E_b/N_0 = 20 \text{ [dB]}$). Both cases use the predistorter.	141
4.9	Channel responses estimated by the new and the conventional LMS algorithm ($\text{OBO}=6 \text{ [dB]}$)	141
4.10	BER performance of coded OFDM systems over an ISI channel	142
4.11	BER performance of the MAP Equaliser in BPSK and a 16-QAM system over an ISI channel	143
4.12	Evolution of the channel estimation according to the number of iterations ($K_{\text{SYM}} = 1000$)	143
4.13	Frequency response of the estimated channel parameters according to the number iterations ($i = 1 \dots 9$)	144
4.14	BER comparison of the MAP equaliser in a known and an unknown channel	145
4.15	BER comparison between MAP equaliser and conventional LMS equaliser.	145
4.16	BER performance of the proposed equaliser (EQ)	146
4.17	BER performance of turbo equalisation over a known and an unknown AWGN and ISI channel according to the number of iterations	147
4.18	Blind channel estimation by EM algorithm for 16-QAM	148
4.19	MSE of blind channel estimation by EM algorithm for 16-QAM	148
4.20	BER performance of the MAP Equaliser for 16-QAM over a multipath channel	150
4.21	Improved BER performance after MAP equalisation through convolutional coding	151

4.22 BER performance of a TTCM equaliser for 16-QAM using Gray mapping over an ISI channel, 2 bits/symbol	152
4.23 BER performance of a TTCM equaliser for 16-QAM over an ISI channel, $K_{\text{SYM}}=800$	152
4.24 BER performance of a TTCM equaliser for 16-QAM over an ISI channel, Block Size ($K_{\text{SYM}}=400, 800$ and 1600)	153
4.25 BER comparison between the proposed approach and other's approaches for TTCM-equalisation	153
4.26 BER comparison of TTCM equalisation between a known channel and an unknown channel	154